HHS Public Access

Author manuscript

Arch Oral Biol. Author manuscript; available in PMC 2022 April 01.

Published in final edited form as:

Arch Oral Biol. 2021 April ; 124: 105067. doi:10.1016/j.archoralbio.2021.105067.

$P2Y_2$ Receptor Antagonism Resolves Sialadenitis and Improves Salivary Flow in a Sjögren's Syndrome Mouse Model

Kimberly J. Jasmer[a,*], **Lucas T. Woods**[a], **Kevin Muñoz Forti**[a], **Adam L. Martin**[a,1], **Jean M. Camden**[a], **Marco Colonna**[b], **Gary A. Weisman**[a]

[a]Department of Biochemistry and Christopher S. Bond Life Sciences Center University of Missouri 1201 Rollins St.Columbia, Missouri, 65211-7310 USA

[b]Department of Pathology and Immunology, Washington University School of Medicine, 660 S. Euclid Ave.St. Louis, MO 63110, USA

Abstract

Objective: Sjögren's syndrome (SS) is a chronic autoimmune exocrinopathy characterized by lymphocytic infiltration of the salivary and lacrimal glands and decreased saliva and tear production. Previous studies indicate that the G protein-coupled $P2Y_2$ nucleotide receptor ($P2Y_2R$) is upregulated in numerous models of salivary gland inflammation (*i.e.* sialadenitis), where it has been implicated as a key mediator of chronic inflammation. Here, we evaluate both systemic and localized $P2Y_2R$ antagonism as a means to resolve sialadenitis in the NOD.H-2^{h4},IFN$\gamma^{-/-}$,$CD28^{-/-}$ (NOD.H-2^{h4} DKO) mouse model of SS.

Design: Female 4.5 month old NOD.H-2^{h4} DKO mice received daily intraperitoneal injections for 10 days of the selective $P2Y_2R$ antagonist, AR-C118925, or vehicle-only control. Single-dose localized intraglandular antagonist delivery into the Wharton's duct was also evaluated. Carbachol-induced saliva was measured and then submandibular glands (SMGs) were isolated and

*Corresponding author: Kimberly Jasmer, JasmerK@missouri.edu.

[1]Present Address: Sinclair Research Center, 562 MO-DD, Auxvasse, MO 65231

Author Contributions:

Kimberly J Jasmer: Conceptualization, Methodology, Investigation, Formal Analysis, Data Curation, Writing – Original Draft, Project Administration, Funding Acquisition

Lucas T Woods: Conceptualization, Methodology, Investigation, Formal Analysis, Validation, Data Curation, Writing – Review & Editing

Kevin Muñoz Forti: Methodology, Investigation, Formal Analysis, Writing – Review & Editing

Adam L Martin: Methodology, Investigation, Formal Analysis, Data Curation, Writing – Review & Editing

Jean M Camden: Conceptualization, Methodology, Investigation, Formal Analysis, Supervision, Validation, Writing – Review & Editing

Marco Colonna: Conceptualization, Funding Acquisition, Writing – Review & Editing

Gary A Weisman: Conceptualization, Funding Acquisition, Supervision, Writing – Review & Editing

Declaration of interests

The authors declare that they have no known competing financial interests or personal relationships that could have appeared to influence the work reported in this paper.

Declarations of interest:

None

either fixed and paraffin-embedded for H&E staining, homogenized for RNA isolation or dissociated for flow cytometry analysis.

Results: Intraperitoneal injection, but not localized intraglandular administration, of AR-C118925 significantly enhanced carbachol-induced salivation and reduced lymphocytic foci and immune cell markers in SMGs of 5 month old NOD.H-2^{h4} DKO mice, compared to vehicle-injected control mice. We found that B cells represent the primary immune cell population in inflamed SMGs of NOD.H-2^{h4} DKO mice that express elevated levels of $P2Y_2R$ compared to controls. We further demonstrate a role for $P2Y_2Rs$ in mediating B cell migration and the release of IgM.

Conclusion: Our findings suggest that the $P2Y_2R$ represents a novel therapeutic target for the treatment of Sjögren's syndrome.

Keywords

Sjögren's syndrome; purinergic receptor; nucleotide; B lymphocytes; autoimmune disease; alarmins

Introduction

SS is an autoimmune exocrinopathy manifested as dry mouth (*i.e.*, xerostomia) and/or dry eye, where chronic exocrine dysfunction can lead to dental caries, swallowing and speech impairment, digestive disorders and vision deterioration that severely reduce the quality of life for patients, 90% of whom are women (Mariette & Criswell, 2018, Maarse *et al.*, 2019). SS is characterized by significant lymphocytic infiltration of the salivary and lacrimal glands, where sustained accumulation of immune cells may lead to glandular destruction and tissue fibrosis (Leehan *et al.*, 2018; Wynn & Ramalingam, 2012). SS patients are also at elevated risk for the development of co-morbidities (Pego-Reigosa *et al.*, 2019), such as secondary autoimmune diseases (*e.g.,* RA, SLE or systemic sclerosis) (Amador-Patarroyo *et al.*, 2012) and lymphoma (Nocturne & Mariette, 2015). Current diagnostic criteria for SS include the presence of immune cell foci in salivary glands (minor salivary gland biopsy focus score of ≥ 1), serum autoantibodies against the ribonucleoprotein Ro/SSA and functional deficits, such as reduced ocular staining and tear and saliva production (Shiboski *et al.*, 2017). Treatment options for xerostomia in SS are limited to symptom management with topical applications, including saliva substitutes and lubricants or cholinergic secretagogues (*e.g.*, pilocarpine and cevimeline) aimed at stimulating secretion from residual functional acinar cells (Fox *et al.,* 2019; Saraux *et. al.,* 2016). These products provide inadequate symptom relief and their utility is further reduced by the incidence of systemic adverse events (Fox *et al.,* 2019; Saraux *et al.,* 2016). Thus, development of more effective SS therapies that treat the underlying chronic inflammation is essential.

Alarmins are endogenous signals released by damaged and dying cells that initiate immune responses involving both the innate and adaptive immune systems (Zindel & Kubes, 2020; Yang *et al.*, 2017). Our laboratory has investigated how localized release of alarmins, such as the cytoplasmic nucleotide adenosine 5'-triphosphate (ATP) from damaged cells or tissues, act to initiate chronic inflammatory responses through activation of P2 purinergic receptors

(Khalafalla *et al.*, 2020; Woods *et al.*, 2018; Khalafalla *et al.*, 2017; Woods *et al.*, 2012). Importantly, blocking alarmin signaling may provide a means to ameliorate the damaging effects of chronic inflammation and preserve salivary gland function in SS (Cao *et al.*, 2019; Khalafalla *et al.*, 2017).

P2 receptors, including the ATP-gated ionotropic P2X receptors and G protein-coupled P2Y receptors, act as sensors for nucleotides released by damaged cells (Khalafalla *et al.*, 2020; Riteau *et al.*, 2012; Woods *et al.*, 2012; Elliott *et al.*, 2009). In salivary gland epithelial cells, the P2X7 receptor (P2X7R) for ATP promotes apoptosis, caspase activation and stimulation of the NLRP3 inflammasome leading to the release of pro-inflammatory cytokines, including IL-1β and IL-18 (Khalafalla *et al.*, 2017; Woods *et al.*, 2012). Previous studies demonstrate that pharmacological antagonism of the P2X7R reduces inflammation and improves salivation in the NOD.H-2^{h4},IFNγ$^{-/-}$,CD28$^{-/-}$ (NOD.H-2^{h4} double knockout; DKO) mouse model of SS (Khalafalla *et al.*, 2017). Notably, our studies have shown that IL-1β increases NF-κB-dependent expression of the G protein-coupled $P2Y_2$ nucleotide receptor ($P2Y_2R$) (Peterson *et al.*, 2013; Degagne *et al.*, 2009; Kong *et al.*, 2009), a well-accepted regulator of localized immune responses (Elliott *et al.*, 2009; Chen *et al.*, 2006) that is activated equipotently by uridine 5'-triphosphate (UTP) or ATP. An NF-κB binding site in the proximal *$P2Y_2R$* promoter upregulates the $P2Y_2R$, which stimulates pro-inflammatory responses in intestinal epithelial cells (Degagne *et al.*, 2009). While not expressed in the salivary glands under physiological conditions, $P2Y_2$Rs are upregulated in several models of sialadenitis, including submandibular gland (SMG) duct ligation-induced inflammation (Ahn *et al.*, 2000) and the NOD.B10 (Schrader *et al.*, 2005) and IL-14αTG mouse models of SS (Woods *et al.*, 2018). Under inflammatory conditions, $P2Y_2R$ signaling has been implicated in the recruitment, migration and proliferation of immune cells (Elliott *et al.*, 2009; Chen *et al.*, 2006) through the activation of numerous signaling pathways, including Src-mediated transactivation of growth factor receptors, interaction with and activation of RGD-binding integrins, activation of the matrix metalloproteases ADAM10 and ADAM17, MAPK activation and canonical $G_q\alpha$ signaling leading to increased intracellular Ca^{2+} levels (Woods *et al.*, 2018; Ratchford *et al.*, 2010; Bagchi *et al.*, 2005; Liu *et al.*, 2004). Furthermore, genetic ablation of *$P2Y_2R$* attenuates sialadenitis in the IL-14αTG mouse model of SS (Woods *et al.*, 2018), suggesting that targeting the ATP-P2X7R-$P2Y_2R$ axis may be an effective therapeutic approach to reduce inflammation and improve salivary function in SS. Here, we utilized the NOD.H-2^{h4} DKO mouse model of SS, which develops significant hyposalivation and sialadenitis by 4 months of age (Voynova *et al.*, 2018; Kayes *et al.*, 2016), to assess the effects of pharmacological $P2Y_2R$ antagonism on sialadenitis by comparing the responses to localized intraglandular versus systemic administration of the selective $P2Y_2R$ antagonist AR-C118925 (Rafehi *et al.*, 2017). Similar to primary SS patients, approximately 50% of NOD.H-2^{h4} DKO mice develop autoimmune thyroid disease in addition to exocrinopathy by 5–6 months of age, whereas supplementation of drinking water with sodium iodide for 2–3 weeks induces severe thyroid disease in all NOD.H-2^{h4} DKO mice (Kayes *et al.*, 2016). Autoimmune thyroid disease is the most common co-existing autoimmune disorder in SS patients (Baldini *et. al*, 2018).

In the IL-14αTG mouse model of SS, we have reported that P2Y2R expression and function are significantly increased in SMG-infiltrating B cells compared to controls and that global

$P2Y_2R$ knockout attenuates the infiltration of B and T lymphocytes into the salivary gland (Woods *et al.*, 2018). Similarly, we report here that SMG-infiltrating B cells in female NOD.H-2^{h4} DKO mice express functional $P2Y_2Rs$. We further demonstrate that $P2Y_2R$ antagonism diminishes B cell migration and IgM secretion *in vitro*. Through the nucleotide-induced activation of $P2Y_2Rs$ on B cells of the SMG, we hypothesize that $P2Y_2Rs$ facilitate the recruitment of peripheral lymphocytes and initiate a chronic immune response in SS resulting in progressive salivary gland inflammation, hyposalivation and secondary effects (*e.g.*, fibrosis, secondary autoimmune conditions and lymphoma). Our findings that systemic $P2Y_2R$ antagonist (*i.e.*, AR-C118925) administration ameliorates sialadenitis and improves saliva flow in NOD.H-2^{h4} DKO mice supports future studies investigating the $P2Y_2R$ as a novel therapeutic target for the treatment of human SS.

Materials and Methods

Mice

C57BL/6 (Jackson Laboratories, Bar Harbor, ME) and NOD.H-2^{h4},IFN$\gamma^{-/-}$,CD$28^{-/-}$ (NOD.H-2^{h4} DKO) mice (Mutant Mouse Resource & Research Center, Columbia, MO) were housed at the Christopher S. Bond Life Sciences Center Animal Facility of the University of Missouri (Columbia, MO), where they received daily welfare assessment by veterinary staff. Mice were housed in vented cages with 12 hr light/dark cycles and received food and water ad libitum. Previous studies indicate that female NOD.H-2^{h4} DKO mice develop more rapid and severe sialadenitis than male mice (Kayes *et al.*, 2016), similar to human SS patients. Therefore, 4.5–5 month old female mice were used for all experiments. All experimental procedures were approved by the University of Missouri Animal Care and Use Committee (Protocol No. 9661) and conducted in accordance with National Institutes of Health guidelines.

Primary SMG B Cell Enrichment

Isolated SMGs from C57BL/6 and NOD.H-2^{h4} DKO mice were minced, placed in RPMI medium with 10% (v/v) FBS, 1% (w/v) penicillin/streptomycin, 4 mg/ml collagenase and 5 mM CaCl2 for 1 hour at 37°C with shaking. Digested SMGs were filtered through a 40 μm nylon filter, centrifuged and resuspended in red blood cell lysis buffer (Miltenyi Biotec, Bergisch Gladbach, Germany). B cells were isolated from the resulting cell suspension by negative selection using the Pan B Cell II Isolation Kit with MACS MS columns (Miltenyi Biotec). Following enrichment, flow cytometry was used to determine that the resulting suspension contains approximately 80% $B220^+$ B cells (REA755, Miltenyi Biotech 130–110-710; 1:50 dilution).

Quantitative Real-Time PCR

For whole SMG tissue preparations, SMGs were excised from euthanized mice and homogenized in TRIzol reagent (ThermoFisher Scientific, Waltham, MA). Chloroform was added to the homogenized tissue (0.2 ml/ml TRIzol), which was then incubated at room temperature for 15 minutes followed by centrifugation at 10,000 x g for 18 minutes at 4°C. RNA was then isolated from the aqueous phase using the RNeasy Plus Mini Kit (Qiagen, Valencia, CA), according to manufacturer's instructions. For enriched B cells, cell pellets

were suspended in Buffer RLT (Qiagen), homogenized by passing through an 18-gauge needle 10 times and RNA was isolated using the RNeasy Plus Mini Kit. cDNA was synthesized from purified RNA using the RNA to cDNA EcoDry Premix (Takara Bio, Mountain View, CA). Quantitative real-time PCR was performed on an Applied Biosystems 7500 Real-Time PCR machine using specific Taqman primers for mouse *$P2Y_2R$*, *GAPDH*, *18S*, *CD3*, *CD20* or *CD45*. Target gene expression was normalized to either *GAPDH* or *18S* ribosomal RNA. qRT-PCR data are shown as either relative expression (Figure 4) compared to a control mouse or ΔCt (Figure 2 and 3), where a higher ΔCt value indicates lower expression. ΔCt is calculated as the Ct of the target gene minus the Ct of the reference gene.

SDS-PAGE and Western Blot Analysis

Isolated B cells were suspended in serum-free RPMI media, incubated with or without 10 μM AR-C118925 at 37°C and 5% CO_2 for 1 hour, then stimulated with 100 μM UTP or 10 μg/ml IgM for 5 minutes before lysis. B cell lysis was achieved using 5X Laemmli Buffer (50 mM sodium phosphate, pH 7.0, 25% (v/v) glycerol, 10% (w/v) SDS, 0.025% (w/v) bromophenol blue and 250 mM DTT). Samples were sonicated, subjected to SDS-PAGE using a 4–20% gradient gel and transferred to nitrocellulose membranes. Membranes were blocked in 5% (w/v) non-fat dry milk dissolved in Tris-buffered saline (pH 7.4) containing 0.1% (v/v) Tween-20 (TBST) for one hour then incubated for 16 h at 4°C with primary antibodies against phosphor-ERK1/2 or total ERK1/2 (Cell Signaling Technology, Danvers, MA; diluted 1:1,000 in TBST). Membranes were washed three times in TBST then incubated with HRP-conjugated anti-mouse IgG antibody (Cell Signaling Technology) for 1 hour at room temperature. Membranes were exposed to SuperSignal West Pico PLUS Chemiluminescent Substrate (ThermoFisher Scientific) and visualized on a UVP BioSpectrum MultiSpectral Imaging System. Protein bands were quantified using Image J and phospho-ERK1/2 expression was normalized to total ERK1/2.

Intracellular Calcium Measurements by Flow Cytometry

SMGs were minced, digested and filtered (as above), then incubated for 20 minutes at 37°C in DMEM containing 10% (v/v) FBS and 3 μM fluo-4 AM (ThermoFisher), a cell-permeant Ca^{2+}-sensitive dye. Cells were then washed with PBS and incubated for 10 minutes at 4°C with anti-B220 APC-conjugated fluorescent antibody (REA755, Miltenyi Biotech 130–110-710; 1:50 dilution). After washing, cells were resuspended in PBS containing 1 mM $CaCl_2$ and analyzed using a BD Biosciences Accuri C6 flow cytometer. After gating for $B220^+$ B cells and obtaining baseline fluo-4 fluorescence (494 nm/516 nm) for 30 seconds, 100 μM UTP was added and the increase in calcium-bound fluo-4 fluorescence corresponding to $\Delta[Ca^{2+}]_i$ was recorded. Where noted, cells were pre-treated with 10 μM AR-C118925 for 5 minutes prior to UTP addition.

Flow Cytometry

SMGs were minced, digested and filtered (as above). Cells were resuspended in PBS containing 0.5% (w/v) BSA and 2 mM EDTA. Single cells were quantified using a Countess II cell counter (Life Technologies) and stained with Viobility Dye 405/520 (Miltenyi Biotech) for 15 minutes at room temperature in the dark, washed, incubated for 5 minutes with FC Block (BD Pharmingen, Franklin Lakes, NJ) and then incubated for 30 minutes at

4°C with fluorophore-conjugated antibodies against CD45 (Vioblue, REA737, Miltenyi Biotech 130–110-664), CD19 (PE-Vio770, REA749, Miltenyi Biotech 130–111-885), F4/80 (FITC, REA126, Miltenyi Biotech 130–102-327) and CD3 (APC, REA606, Miltenyi Biotech 130–109-240) for immunophenotyping by flow cytometry using a BD LSRFortessa Cell Analyzer. Spectral compensation was established with Ultracomp eBeads (Invitrogen, Carlsbad, CA). A representative gating strategy is shown in Supplementary Figure S1. Fluorescence minus one samples for all antibodies were used as gating controls. Data were analyzed using FlowJo v10.5.0 software.

Transwell Migration Assay

Isolated SMG B cells were treated with or without 10 μM AR-C118925 for 1 hour at 37°C and 5% CO_2. Then, 2×10^5 cells in RPMI media containing 0.1% FBS were seeded in the upper well of a 5 μm pore Transwell chamber, while the lower chamber was filled with RPMI media containing 0.1% FBS and either UTP (100 μM) or CXCL12 (50 ng/ml). After 4 hours, cells that migrated through the pores and entered the lower chamber were collected by centrifugation and enumerated.

IgM ELISA

Isolated SMG B cells (5×10^5 cells per sample) were plated in a 96-well plate with 100 μl complete RPMI medium and pre-treated with or without 10 μM AR-C118925 for 1 hour prior to treatment with either 100 μM UTP or 1 μM PMA for 72 hours at 37°C and 5% CO_2. The 96-well plate was then briefly spun and 80 μl of supernatant collected. Forty μl of the undiluted supernatant was used to measure IgM concentrations using a mouse IgM uncoated ELISA kit (ThermoFisher).

In Vivo Antagonist Studies

For intraglandular delivery, mice were anesthetized with tribromoethanol (Avertin, 0.3 mg/g body weight). Then, 30 μl of either 100 μM AR-C118925 or vehicle (saline) was injected into the Wharton's ducts using a 31-gauge syringe. Efficiency of delivery can be visualized in Supplementary Figure S2. Three days later, mice were anesthetized and an endotracheal tube (PE50 polyethylene tubing) was inserted through a midventral incision at the base of the throat. Whole saliva was collected from the oral cavity for 15 minutes following intraperitoneal (i.p.) injection of carbachol (0.25 mg/kg body weight), as previously described (Kayes *et al.*, 2016). For systemic treatment, 1 mg/kg/day AR-C118925 or vehicle (corn oil) was administered daily via i.p. injection over 10 days before carbachol-induced saliva collection was performed. Mice were then euthanized by cervical dislocation and SMGs were excised and prepared for histological analysis, qRT-PCR or FACS analysis. For all experiments, littermates housed in the same cages served as controls.

Immunohistochemistry and Focus Score Measurement

Excised SMGs were fixed in 4% (w/v) paraformaldehyde in PBS at 4°C for 24 hours. Samples were then sent to IDEXX Laboratories (Columbia, MO), where formaldehyde-fixed paraffin-embedded sections were stained with hematoxylin and eosin or with anti-CD3 (Agilent, Santa Clara, CA) or anti-B220 (Invitrogen) antibodies to identify T or B cells,

respectively. Stained sections were visualized on a Zeiss Axiovert 200M inverted microscope at the University of Missouri Molecular Cytology Core Facility. To generate images of whole SMG sections, multiple 10X bright-field images were stitched together using MetaMorph software. Lymphocytic foci were then enumerated and the total glandular area was determined using MetaMorph software. Focus scores were calculated as the number of lymphocytic foci per 4 mm^2 of glandular area, as described (Daniels *et al.*, 2011).

Statistics

Quantitative results are shown as mean ± S.E.M. and are representative of three or more independent experiments. Statistical significance was determined by standard Student's t-test. All statistical analyses were performed using GraphPad Prism 7 software.

Results

B and T lymphocytes are the predominant immune cell populations in NOD.H-2^{h4} DKO mouse submandibular gland

Compared to age-matched female C57BL/6 mice, 5 month old NOD.H-2^{h4} DKO mice develop substantial immune cell accumulation in the submandibular glands that is composed primarily of B and T lymphocytes (Figure 1). Flow cytometric analysis of $CD45^+$ immune cells isolated from the SMG revealed that greater than 50% were $CD19^+$ B lymphocytes with $CD3^+$ T lymphocytes comprising nearly 40% (Figure 1A). The proportion of $CD45^+$ immune cells that were $F4/80^+$ macrophages was significantly decreased in NOD.H-2^{h4} DKO mice compared to age-matched C57BL/6 mice, likely because of the robust accumulation of B and T lymphocytes (Figure 1A). Histological analysis of H&E-, anti-CD3- or anti-B220-stained SMG sections revealed large lymphocytic foci with striking organization of B and T cells in 5 month old female NOD.H-2^{h4} DKO mice (Figure 1B and 1C).

Systemic, but not localized, administration of AR-C118925 diminishes sialadenitis and improves salivation in NOD.H-2^{h4} DKO mice

To determine the *in vivo* effects of $P2Y_2R$ antagonism on sialadenitis and hyposalivation in NOD.H-2^{h4} DKO mice, we compared the local administration of AR-C118925 via intraglandular retrograde infusion of the submandibular gland (Figure 2) versus systemic administration via intraperitoneal injection (Figure 3). For intraglandular administration, 30 μl of 100 μM AR-C118925 in saline was infused directly through the Wharton's ducts of 4.5 month old female NOD.H-2^{h4} DKO mice. After 3 days, histological analysis of H&E-stained SMG sections revealed that intraglandular administration of AR-C118925 compared to saline had no effect on lymphocyte focus score (Figure 2A and 2B), which is defined as the number of lymphocytic foci per 4 mm^2 of glandular area (Daniels *et al.*, 2011). Also, qRT-PCR of cDNA prepared from whole SMGs showed no significant differences in expression of the immune cell markers *CD45* (total immune cells), *CD20* (B cells) or *CD3* (T cells) in the presence or absence of AR-C118925 (Figure 2C). While qRT-PCR did not identify a significant change in B and T cell markers, flow cytometric analysis of $CD45^+$ immune cells isolated from the SMG revealed a significant decrease in the proportion of $CD19^+$ B cells and a compensatory increase in $CD3^+$ T cells with AR-C118925 compared to

saline treatment (Figure 2D). Intraglandular administration of AR-C118925 did not improve carbachol-induced saliva secretion (Figure 2E) and a significant inverse correlation between saliva volume and focus score was observed (Figure 2F) for both AR-C118925- and saline-treated mice.

Systemic administration of AR-C118925 (1 mg/kg/day) via intraperitoneal injection for 10 days significantly reduced focus score in 4.5 month old female NOD.H-2^{h4} DKO mice, as compared to corn oil (vehicle)-injected control mice (Figure 3A and 3B). Furthermore, qRT-PCR of cDNA prepared from whole SMGs revealed a significant decrease in *CD45*, *CD20* and *CD3* expression, indicating a reduction in total immune cells, B cells and T cells, respectively (Figure 3C). Whereas intraglandular AR-C118925 administration decreased the proportion of $CD19^+$ B cells in SMGs compared to vehicle injection, i.p. AR-C118925 administration had no effect on the relative proportions of B cells, T cells and macrophages (Figure 3D). While the total immune cell burden in the SMG decreased (Figure 3B and 3C) the composition of the immune cells that remain did not significantly change, at least in terms of the relative proportion of B cells, T cells, and macrophages (Figure 3D). Notably, carbachol-induced saliva production was significantly increased in systemic AR-C118925-treated mice compared to vehicle-treated controls (Figure 3E) and a significant inverse correlation between saliva volume and focus score was observed for both AR-C118925- and vehicle-treated mice (Figure 3F).

Submandibular gland B cells express functional $P2Y_2Rs$

As our previous studies using the IL-14αTG mouse model of SS demonstrated increased $P2Y_2R$ function in SMG-infiltrating B cells compared to controls (Woods *et al.*, 2018), we assayed $P2Y_2R$ expression and function in B and T cells isolated from 5 month old female NOD.H-2^{h4} DKO or C57BL/6 mouse SMG. Quantitative real-time PCR revealed significant *$P2Y_2R$* upregulation in SMG B cells isolated from NOD.H-2^{h4} DKO mice, as compared to age-matched C57BL/6 mice (Figure 4A). As $P2Y_2R$ activation by extracellular ATP or UTP stimulates canonical G_q signaling leading to Ca^{2+} release from intracellular stores, UTP-induced changes in $[Ca^{2+}]_i$ were assayed by flow cytometric analysis using the cell permeant Ca^{2+}-sensitive dye Fluo-4 AM. Enzymatically-dispersed SMG cells were loaded with Fluo-4 AM, labeled with fluorescent anti-B220-APC antibodies to detect B cells and continuous Fluo-4 fluorescence was measured in $B220^+$ cells. UTP (100 μM) induced a marked, yet transient increase in $[Ca^{2+}]_i$ that was abrogated by a 5 minute pre-treatment with the selective $P2Y_2R$ antagonist AR-C118925 (10 μM) (Figure 4B). In contrast, UTP-induced changes in $[Ca^{2+}]_i$ were undetectable in SMG or splenic T cells isolated from NOD.H-2^{h4} DKO mice (Supplementary Figure S3), suggesting that $P2Y_2Rs$ are not expressed in SMG-infiltrating T cells.

Because $P2Y_2R$ activation stimulates MAPK (*i.e.*, ERK1/2) phosphorylation (Ratchford *et al.*, 2010), UTP-induced ERK1/2 phosphorylation was also determined to assess $P2Y_2R$ activity. B cells isolated from the SMG of 5 month old female NOD.H-2^{h4} DKO mice treated with 100 μM UTP for five minutes show significantly elevated ERK1/2 phosphorylation that was attenuated by pre-treatment with AR-C118925 (10 μM) for one hour (Figure 4C). Interestingly, AR-C118925 caused a significant, though modest decrease

in basal activity, suggesting constitutive activation of $P2Y_2R$, as well as UTP-induced ERK1/2 phosphorylation. To ensure the diminished ERK1/2 phosphorylation observed following AR-C118925 treatment was not a result of loss of cell viability, an XTT assay was conducted on primary B cells which demonstrated no loss of cell viability (Supplementary Figure S4). IgM (10 μg/ml), which crosslinks and activates the B cell receptor leading to ERK1/2 phosphorylation through activation of the Ras, phospholipase C (PLC) and phosphoinositide 3- (PI3)-kinase signaling pathways (Jacob *et al.*, 2002), was used as a positive control for ERK1/2 activation.

UTP-induced B cell migration and IgM secretion is attenuated by AR-C118925

We hypothesized that $P2Y_2Rs$ expressed by SMG B lymphocytes contribute to SS pathogenesis by facilitating B cell recruitment or migration to the SMG. We demonstrate that UTP (100 μM) added to the lower chamber in a Transwell migration assay significantly enhanced B cell migration from the upper chamber that was attenuated by pre-treatment of the cells with 10 μM AR-C118925 (Figure 4D). CXCL12 (50 ng/ml), a well-accepted mediator of B cell migration, was used as a positive control. Although B lymphocytes fulfill a number of functions, including regulatory roles, the major function of a B cell is antibody production (LeBien & Tedder, 2008). To assess whether $P2Y_2R$ activity contributes to the secretion of immunoglobulin M (IgM), we measured IgM in the cell culture medium of isolated SMG B lymphocytes by ELISA (Figure 4E). We found that treatment with UTP (100 μM) for 72 hours significantly increased the secretion of IgM from isolated B cells, a response that was abrogated by a 1 hour pre-treatment with 10 μM AR-C118925. As expected, the protein kinase C (PKC) activator phorbol myristate acetate (PMA; 1 μM) significantly increased PKC-mediated IgM release.

Discussion

Among the ever-increasing list of endogenous alarmins, extracellular ATP released from damaged or dying cells promotes production of pro-inflammatory cytokines and chemokines, activation of macrophages and dendritic cells and leukocyte recruitment through P2 receptor signaling (Yang *et al.*, 2017; Riteau *et al.*, 2012; Woods *et al.*, 2012; Elliott *et al.*, 2009). P2 receptor antagonism has been investigated in pre-clinical studies and clinical trials for the treatment of a number of inflammatory and autoimmune conditions (Burnstock, 2017; Khalafalla *et al.*, 2020). We have previously reported that antagonism of P2X7R or genetic ablation of $P2Y_2R$ resolves sialadenitis and improves salivary function in NOD.H-2^{h4} DKO (Khalafalla *et al.*, 2017) and IL-14αTG (Woods *et al.*, 2018) mouse models of Sjögren's syndrome, respectively. Here, we demonstrate that systemic pharmacological blockade of the $P2Y_2R$ by AR-C118925 using multiple i.p. injections in NOD.H-2^{h4} DKO mice diminishes sialadenitis in SMGs and enhances carbachol-induced saliva secretion (Figure 3). In contrast, localized delivery of a single dose of AR-C118925 via the Wharton's duct had little effect on saliva secretion (Figure 2). Nonetheless, sialendoscopic irrigation of the salivary gland followed by intraductal administration of anti-inflammatory drugs is a promising avenue for SS treatment (Karagozoglu *et al.*, 2018), so future studies should examine whether multiple intraductal injections of AR-C118925 will be efficacious in diminishing sialadenitis, while minimizing off-target effects that are more

likely with systemic administration. NOD.H-2^{h4} DKO mice demonstrate variability in the extent of sialadenitis, which inversely correlates with saliva production, suggesting that the pathogenesis of hyposalivation in NOD.H-2^{h4} DKO mice is dependent on SMG inflammation. This relationship remains whether mice are treated with AR-C118925 or vehicle only, consistent with a mechanism by which AR-C118925 treatment improves saliva flow by reducing inflammation in the gland, which we report here.

Because SS is characterized by several indicators of B cell dysfunction (Ambrus *et. al*, 2016; Ibrahem, 2019), we investigated whether B cells that accumulate in the SMGs of NOD.H-2^{h4} DKO mice exhibit functional $P2Y_2R$ expression that contributes to SS pathogenesis. Indeed, isolated SMG B cells from NOD.H-2^{h4} DKO mice have increased $P2Y_2R$ expression, as compared to SMG B cells from non-inflamed C57BL/6 mice, and exhibit UTP-induced increases in $[Ca^{2+}]_i$ and ERK1/2 phosphorylation that are blocked by AR-C118925 (Figure 4). We further show that UTP enhances B cell migration and secretion of IgM, responses that were abolished by $P2Y_2R$ antagonism (Figure 4). IgM is produced primarily by B-1 cells but is also secreted from activated conventional B-2 cells (Blandino & Baumgarth, 2019). The relevance of IgM in the pathogenesis of autoimmune conditions, including SS, is debated. While some have reported an important role for IgM in autoimmune pathogenesis in both humans and mice (Aziz *et al.,* 2015; Duan & Morel, 2006; Morris *et al.*, 2019), others have demonstrated a protective role for secreted IgM in autoimmunity (Blandino & Baumgarth, 2019; Boes *et al.*, 2000).

The mechanisms by which $P2Y_2Rs$ expressed in SMG B cells contribute to SS pathogenesis may differ in various B lymphocyte subpopulations, although we did not investigate specific B cell subtypes. For example, it has been reported that specific *in vivo* depletion of marginal zone (MZ) B cells ameliorates SS-like symptoms in IL-14αTG mice (Shen *et al.*, 2016). MZ B cells accumulate in the salivary glands of SS patients (Daridon *et al.*, 2006) and most lymphomas that develop in conjunction with SS are derived from MZ B cells (Nocturne & Mariette, 2015), suggesting that these cells play an important role in SS pathogenesis. It would be interesting to determine whether $P2Y_2Rs$ are specifically expressed in MZ B cells and how $P2Y_2R$ antagonism affects this population of B cells in SS models. Despite the body of evidence implicating B cells in SS pathogenesis, B cell depletion using Rituximab has been largely ineffective as a therapeutic strategy (Letaief *et al.*, 2018), possibly due to co-depletion of anti-inflammatory B regulatory cells that are elevated in human SS patients (Mielle *et al.*, 2019). Another explanation for the lack of Rituximab efficacy may be that it fails to deplete long-lived plasma cells (Mahevas *et al.*, 2013; Rosenberg *et al.,* 2016).

The exciting *in vivo* findings that both P2X7R (Khalafalla et al., 2017) and $P2Y_2R$ antagonism (shown here) ameliorate SS-related hyposalivation and resolve lymphocytic infiltration in the salivary glands of NOD.H-2^{h4} DKO mice support targeting the ATP-P2X7R-$P2Y_2R$ axis as a therapeutic strategy for the treatment of SS in humans.

Supplementary Material

Refer to Web version on PubMed Central for supplementary material.

Acknowledgments

Funding:

This work was supported by grants from the National Institutes of Health, R01DE007389 (GAW) and RO1DE025884 (MC, GAW), and a Sjögrens Syndrome Foundation grant (KJ).

Abbreviations:

$P2Y_2R$	$P2Y_2$ receptor
IFNγ	interferon gamma
P2X7R	P2X7 receptor
SMG	submandibular gland
SS	Sjögren's syndrome
UTP	uridine 5'-triphosphate

References

Ahn JS, Camden JM, Schrader AM, Redman RS, & Turner JT (2000). Reversible regulation of P2Y(2) nucleotide receptor expression in the duct-ligated rat submandibular gland. Am J Physiol Cell Physiol, 279(2), C286–294. doi:10.1152/ajpcell.2000.279.2.C286 [PubMed: 10912994]

Amador-Patarroyo MJ, Arbelaez JG, Mantilla RD, Rodriguez-Rodriguez A, Cardenas-Roldan J, Pineda-Tamayo R, … Anaya JM (2012). Sjogren's syndrome at the crossroad of polyautoimmunity. J Autoimmun, 39(3), 199–205. doi:10.1016/j.jaut.2012.05.008 [PubMed: 22749530]

Ambrus JL, Suresh L, & Peck A (2016). Multiple roles for B-lymphocytes in Sjogren's syndrome. J Clin Med, 5(10), 87. doi:10.3390/jcm5100087

Aziz M, Holodick NE, Rothstein TL, & Wang P (2015). The role of B-1 cells in inflammation. Immunol Res, 63(1–3), 153–166. doi:10.1007/s12026-015-8708-3 [PubMed: 26427372]

Bagchi S, Liao Z, Gonzalez FA, Chorna NE, Seye CI, Weisman GA, & Erb L (2005). The P2Y2 nucleotide receptor interacts with alphav integrins to activate Go and induce cell migration. J Biol Chem, 280(47), 39050–39057. doi:10.1074/jbc.M504819200 [PubMed: 16186116]

Baldini C, Ferro F, Mosca M, Fallahi P, & Antonelli A (2018). The association of Sjogren syndrome and autoimmune thyroid disorders. Front Endocrinol (Lausanne), 9, 121. doi:10.3389/fendo.2018.00121 [PubMed: 29666604]

Blandino R, & Baumgarth N (2019). Secreted IgM: New tricks for an old molecule. J Leukoc Biol, 106(5), 1021–1034. doi:10.1002/JLB.3RI0519-161R [PubMed: 31302940]

Boes M, Schmidt T, Linkemann K, Beaudette BC, Marshak-Rothstein A, & Chen J (2000). Accelerated development of IgG autoantibodies and autoimmune disease in the absence of secreted IgM. Proc Natl Acad Sci U S A, 97(3), 1184–1189. doi:10.1073/pnas.97.3.1184 [PubMed: 10655505]

Burnstock G (2017). Purinergic signalling: therapeutic developments. Front Pharmacol, 8, 661. doi:10.3389/fphar.2017.00661 [PubMed: 28993732]

Cao F, Hu LQ, Yao SR, Hu Y, Wang DG, Fan YG, … Wu GC (2019). P2X7 receptor: A potential therapeutic target for autoimmune diseases. Autoimmun Rev, 18(8), 767–777. doi:10.1016/j.autrev.2019.06.009 [PubMed: 31181327]

Chen Y, Corriden R, Inoue Y, Yip L, Hashiguchi N, Zinkernagel A, … Junger WG (2006). ATP release guides neutrophil chemotaxis via P2Y2 and A3 receptors. Science, 314(5806), 1792–1795. doi:10.1126/science.1132559 [PubMed: 17170310]

Daniels TE, Cox D, Shiboski CH, Schiodt M, Wu A, Lanfranchi H, … Sjogren's International Collaborative Clinical Alliance Research, G. (2011). Associations between salivary gland

histopathologic diagnoses and phenotypic features of Sjogren's syndrome among 1,726 registry participants. Arthritis Rheum, 63(7), 2021–2030. doi:10.1002/art.30381 [PubMed: 21480190]

Daridon C, Pers JO, Devauchelle V, Martins-Carvalho C, Hutin P, Pennec YL, … Youinou P (2006). Identification of transitional type II B cells in the salivary glands of patients with Sjogren's syndrome. Arthritis Rheum, 54(7), 2280–2288. doi:10.1002/art.21936 [PubMed: 16802367]

Degagne E, Grbic DM, Dupuis AA, Lavoie EG,… Weisman GA, Sévigny J, & Gendron FP (2009). P2Y2 receptor transcription is increased by NF-kappa B and stimulates cyclooxygenase-2 expression and PGE2 released by intestinal epithelial cells. J Immunol, 183(7), 4521–4529. doi:10.4049/jimmunol.0803977 [PubMed: 19734210]

Duan B, & Morel L (2006). Role of B-1a cells in autoimmunity. Autoimmun Rev, 5(6), 403–408. doi:10.1016/j.autrev.2005.10.007 [PubMed: 16890894]

Elliott MR, Chekeni FB, Trampont PC, Lazarowski ER, Kadl A, Walk SF, … Ravichandran KS (2009). Nucleotides released by apoptotic cells act as a find-me signal to promote phagocytic clearance. Nature, 461(7261), 282–286. doi:10.1038/nature08296 [PubMed: 19741708]

Fox RI, Fox CM, Gottenberg JE, & Dorner T (2019). Treatment of Sjogren's syndrome: current therapy and future directions. Rheumatology (Oxford). doi:10.1093/rheumatology/kez142

Ibrahem HM (2019). B cell dysregulation in primary Sjogren's syndrome: A review. Jpn Dent Sci Rev, 55(1), 139–144. doi:10.1016/j.jdsr.2019.09.006 [PubMed: 31687053]

Jacob A, Cooney D, Pradhan M, & Coggeshall KM (2002). Convergence of signaling pathways on the activation of ERK in B cells. J Biol Chem, 277(26), 23420–23426. doi:10.1074/jbc.M202485200 [PubMed: 11976336]

Karagozoglu KH, Vissink A, Forouzanfar T, Brand HS, Maarse F, & Jager DHJ (2018). Sialendoscopy enhances salivary gland function in Sjogren's syndrome: a 6-month follow-up, randomised and controlled, single blind study. Ann Rheum Dis, 77(7), 1025–1031. doi:10.1136/annrheumdis-2017-212672 [PubMed: 29475854]

Kayes TD, Weisman GA, Camden JM, Woods LT, Bredehoeft C, Downey EF, … Braley-Mullen H (2016). New murine model of early onset autoimmune thyroid disease/hypothyroidism and autoimmune exocrinopathy of the salivary gland. J Immunol, 197(6), 2119–2130. doi:10.4049/jimmunol.1600133 [PubMed: 27521344]

Khalafalla MG, Woods LT, Camden JM, Khan AA, Limesand KH, Petris MJ, … Weisman GA (2017). P2X7 receptor antagonism prevents IL-1beta release from salivary epithelial cells and reduces inflammation in a mouse model of autoimmune exocrinopathy. J Biol Chem, 292(40), 16626–16637. doi:10.1074/jbc.M117.790741 [PubMed: 28798231]

Khalafalla MG, Woods LT, Jasmer KJ, Forti KM, Camden JM, Jensen JL, … Weisman GA (2020). P2 receptors as therapeutic targets in the salivary gland: from physiology to dysfunction. Front Pharmacol, 11, 222. doi:10.3389/fphar.2020.00222 [PubMed: 32231563]

Kong Q, Peterson TS, Baker O, Stanley E, Camden J, Seye CI, … Weisman GA (2009). Interleukin-1beta enhances nucleotide-induced and alpha-secretase-dependent amyloid precursor protein processing in rat primary cortical neurons via up-regulation of the P2Y(2) receptor. J Neurochem, 109(5), 1300–1310. doi:10.1111/j.1471-4159.2009.06048.x [PubMed: 19317852]

LeBien TW, & Tedder TF (2008). B lymphocytes: how they develop and function. Blood, 112(5), 1570–1580. doi:10.1182/blood-2008-02-078071 [PubMed: 18725575]

Leehan KM, Pezant NP, Rasmussen A, Grundahl K, Moore JS, Radfar L, … Farris AD (2018). Minor salivary gland fibrosis in Sjogren's syndrome is elevated, associated with focus score and not solely a consequence of aging. Clin Exp Rheumatol, 36 Suppl 112(3), 80–88. Retrieved from https://www.ncbi.nlm.nih.gov/pubmed/29148407

Letaief H, Lukas C, Barnetche T, Gaujoux-Viala C, Combe B, & Morel J (2018). Efficacy and safety of biological DMARDs modulating B cells in primary Sjogren's syndrome: Systematic review and meta-analysis. Joint Bone Spine, 85(1), 15–22. doi:10.1016/j.jbspin.2017.06.004 [PubMed: 28673789]

Liu J, Liao Z, Camden J, Griffin KD, Garrad RC, Santiago-Perez LI, … Erb L (2004). Src homology 3 binding sites in the P2Y2 nucleotide receptor interact with Src and regulate activities of Src, proline-rich tyrosine kinase 2, and growth factor receptors. J Biol Chem, 279(9), 8212–8218. doi:10.1074/jbc.M312230200 [PubMed: 14670955]

Maarse F, Jager DHJ, Alterch S, Korfage A, Forouzanfar T, Vissink A, & Brand HS (2019). Sjogren's syndrome is not a risk factor for periodontal disease: a systematic review. Clin Exp Rheumatol, 37 Suppl 118(3), 225–233. Retrieved from https://www.ncbi.nlm.nih.gov/pubmed/31464667 [PubMed: 31464667]

Mahevas M, Michel M, Weill JC, & Reynaud CA (2013). Long-lived plasma cells in autoimmunity: lessons from B-cell depleting therapy. Front Immunol, 4, 494. doi:10.3389/fimmu.2013.00494 [PubMed: 24409184]

Mariette X, & Criswell LA (2018). Primary Sjogren's Syndrome. N Engl J Med, 378(10), 931–939. doi:10.1056/NEJMcp1702514 [PubMed: 29514034]

Mielle J, Tison A, Cornec D, Le Pottier L, Daien C, & Pers JO (2019). B cells in Sjogren's syndrome: from pathophysiology to therapeutic target. Rheumatology (Oxford). doi:10.1093/rheumatology/key332

Morris G, Puri BK, Olive L, Carvalho AF, Berk M, & Maes M (2019). Emerging role of innate B1 cells in the pathophysiology of autoimmune and neuroimmune diseases: Association with inflammation, oxidative and nitrosative stress and autoimmune responses. Pharmacol Res, 148, 104408. doi:10.1016/j.phrs.2019.104408 [PubMed: 31454534]

Nocturne G, & Mariette X (2015). Sjogren Syndrome-associated lymphomas: an update on pathogenesis and management. Br J Haematol, 168(3), 317–327. doi:10.1111/bjh.13192 [PubMed: 25316606]

Pego-Reigosa JM, Restrepo Velez J, Baldini C, & Rua-Figueroa Fernandez de Larrinoa I (2019). Comorbidities (excluding lymphoma) in Sjogren's syndrome. Rheumatology (Oxford). doi:10.1093/rheumatology/key329

Peterson TS, Thebeau CN, Ajit D, Camden JM, Woods LT, Wood WG, … Weisman GA (2013). Up-regulation and activation of the P2Y(2) nucleotide receptor mediate neurite extension in IL-1beta-treated mouse primary cortical neurons. J Neurochem, 125(6), 885–896. doi:10.1111/jnc.12252 [PubMed: 23550835]

Rafehi M, Burbiel JC, Attah IY, Abdelrahman A, & Muller CE (2017). Synthesis, characterization, and in vitro evaluation of the selective P2Y2 receptor antagonist AR-C118925. Purinergic Signal, 13(1), 89–103. doi:10.1007/s11302-016-9542-3 [PubMed: 27766552]

Ratchford AM, Baker OJ, Camden JM, Rikka S, Petris MJ, Seye CI, … Weisman GA (2010). P2Y2 nucleotide receptors mediate metalloprotease-dependent phosphorylation of epidermal growth factor receptor and ErbB3 in human salivary gland cells. J Biol Chem, 285(10), 7545–7555. doi:10.1074/jbc.M109.078170 [PubMed: 20064929]

Riteau N, Baron L, Villeret B, Guillou N, Savigny F, Ryffel B, … Couillin I (2012). ATP release and purinergic signaling: a common pathway for particle-mediated inflammasome activation. Cell Death Dis, 3, e403. doi:10.1038/cddis.2012.144 [PubMed: 23059822]

Rosenberg AS, Pariser AR, Diamond B, Yao L, Turka LA, Lacana E, & Kishnani PS (2016). A role for plasma cell targeting agents in immune tolerance induction in autoimmune disease and antibody responses to therapeutic proteins. Clin Immunol, 165, 55–59. doi:10.1016/j.clim.2016.02.009 [PubMed: 26928739]

Saraux A, Pers JO, & Devauchelle-Pensec V (2016). Treatment of primary Sjogren syndrome. Nat Rev Rheumatol, 12(8), 456–471. doi:10.1038/nrrheum.2016.100 [PubMed: 27411907]

Schrader AM, Camden JM, & Weisman GA (2005). P2Y2 nucleotide receptor up-regulation in submandibular gland cells from the NOD.B10 mouse model of Sjogren's syndrome. Arch Oral Biol, 50(6), 533–540. doi:10.1016/j.archoralbio.2004.11.005 [PubMed: 15848146]

Shen L, Gao C, Suresh L, Xian Z, Song N, Chaves LD, … Ambrus JL Jr. (2016). Central role for marginal zone B cells in an animal model of Sjogren's syndrome. Clin Immunol, 168, 30–36. doi:10.1016/j.clim.2016.04.008 [PubMed: 27140729]

Shiboski CH, Shiboski SC, Seror R, Criswell LA, Labetoulle M, Lietman TM, … International Sjogren's Syndrome Criteria Working Group (2017). 2016 American College of Rheumatology/European League Against Rheumatism Classification Criteria for Primary Sjogren's Syndrome: A Consensus and Data-Driven Methodology Involving Three International Patient Cohorts. Arthritis Rheumatol, 69(1), 35–45. doi:10.1002/art.39859 [PubMed: 27785888]

Voynova E, Mahmoud T, Woods LT, Weisman GA, Ettinger R, & Braley-Mullen H (2018). Requirement for CD40/CD40L interactions for development of autoimmunity differs depending on specific checkpoint and costimulatory pathways. Immunohorizons, 2(1), 54–66. doi:10.4049/immunohorizons.1700069 [PubMed: 30607385]

Woods LT, Camden JM, Batek JM, Petris MJ, Erb L, & Weisman GA (2012). P2X7 receptor activation induces inflammatory responses in salivary gland epithelium. Am J Physiol Cell Physiol, 303(7), C790–801. doi:10.1152/ajpcell.00072.2012 [PubMed: 22875784]

Woods LT, Camden JM, Khalafalla MG, Petris MJ, Erb L, Ambrus JL Jr., & Weisman GA (2018). P2Y2 R deletion ameliorates sialadenitis in IL-14alpha-transgenic mice. Oral Dis, 24(5), 761–771. doi:10.1111/odi.12823 [PubMed: 29297959]

Wynn TA, & Ramalingam TR (2012). Mechanisms of fibrosis: therapeutic translation for fibrotic disease. Nat Med, 18(7), 1028–1040. doi:10.1038/nm.2807 [PubMed: 22772564]

Yang, Han Z, & Oppenheim JJ (2017). Alarmins and immunity. Immunol Rev, 280(1), 41–56. doi:10.1111/imr.12577 [PubMed: 29027222]

Zindel J, & Kubes P (2020). DAMPs, PAMPs, and LAMPs in Immunity and Sterile Inflammation. Annu Rev Pathol, 15, 493–518. doi:10.1146/annurev-pathmechdis-012419-032847 [PubMed: 31675482]

Highlights

- Systemic administration of the selective $P2Y_2$ receptor ($P2Y_2R$) antagonist, AR-C118925, resolves salivary gland inflammation and improves saliva flow in the NOD.H-2^{h4},IFN$\gamma^{-/-}$,$CD28^{-/-}$ mouse model of Sjögren's syndrome.
- Single-dose localized administration of AR-C118925 did not resolve inflammation or affect saliva flow in NOD.H-2^{h4},IFN$\gamma^{-/-}$,$CD28^{-/-}$ mice.
- Functional $P2Y_2Rs$ are expressed in isolated salivary gland B lymphocytes
- $P2Y_2Rs$ expressed in salivary gland B lymphocytes promote migration and IgM secretion.

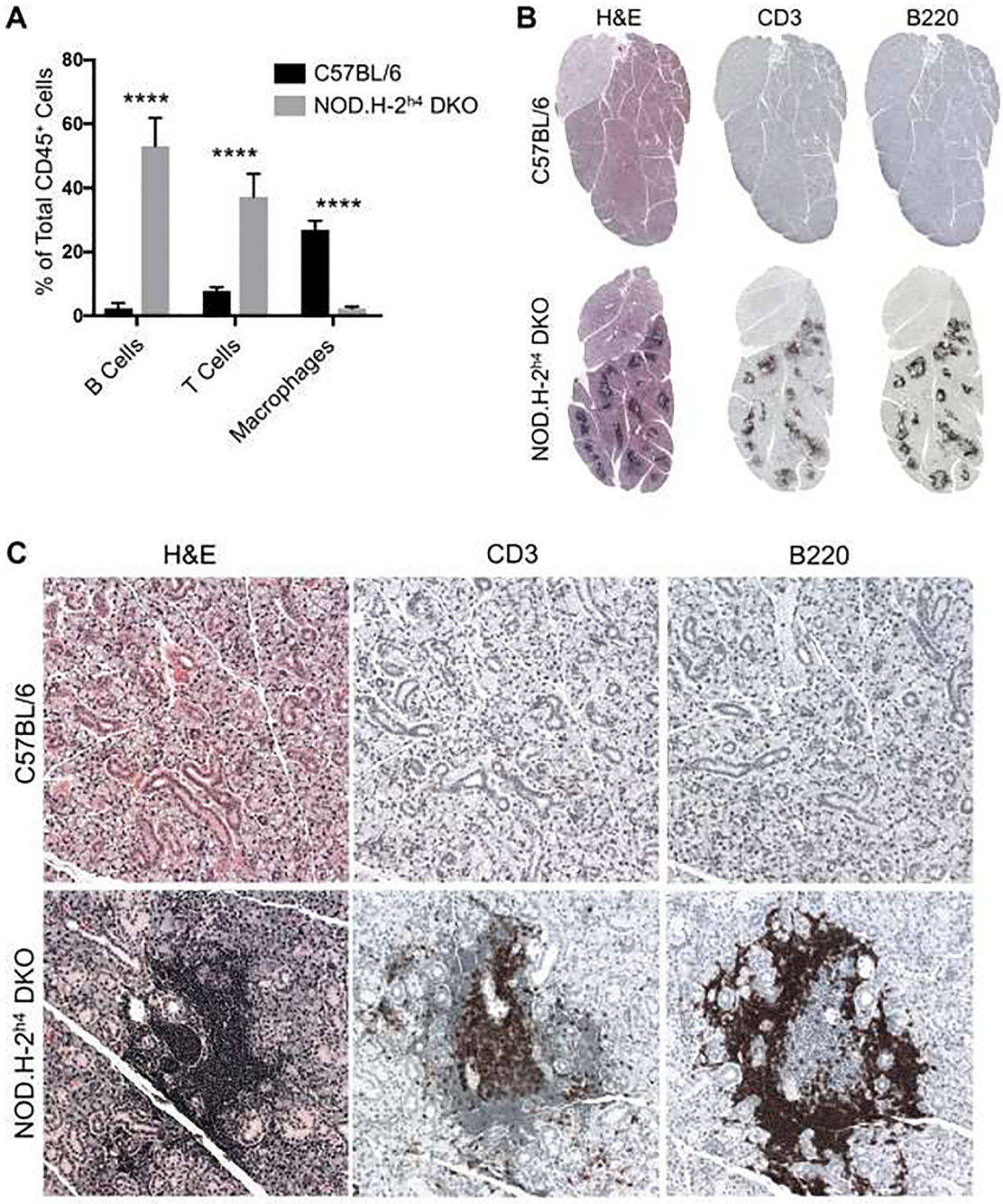

Figure 1. B and T lymphocytes are the predominant immune cell populations in submandibular glands of NOD.H-2^{h4} DKO mice.

(A) Immune cells isolated from SMGs of 5 month old female NOD.H-2^{h4} DKO and C57BL/6 mice were stained with a panel of fluorophore-conjugated antibodies to identify B Cells (CD45$^+$,CD19$^+$), T cells (CD45$^+$,CD3$^+$) and macrophages (CD45$^+$,F4/80$^+$) by flow cytometric analysis. (B and C) Formaldehyde-fixed, paraffin-embedded SMG sections from 5 month old NOD.H-2^{h4} DKO and C57BL/6 mice stained with H&E, anti-CD3 (T cell marker) or anti-B220 (B cell marker) antibodies. Data represent means ± S.E.M. for n = 4 or 5 mice, where ****$P < 0.0001$.

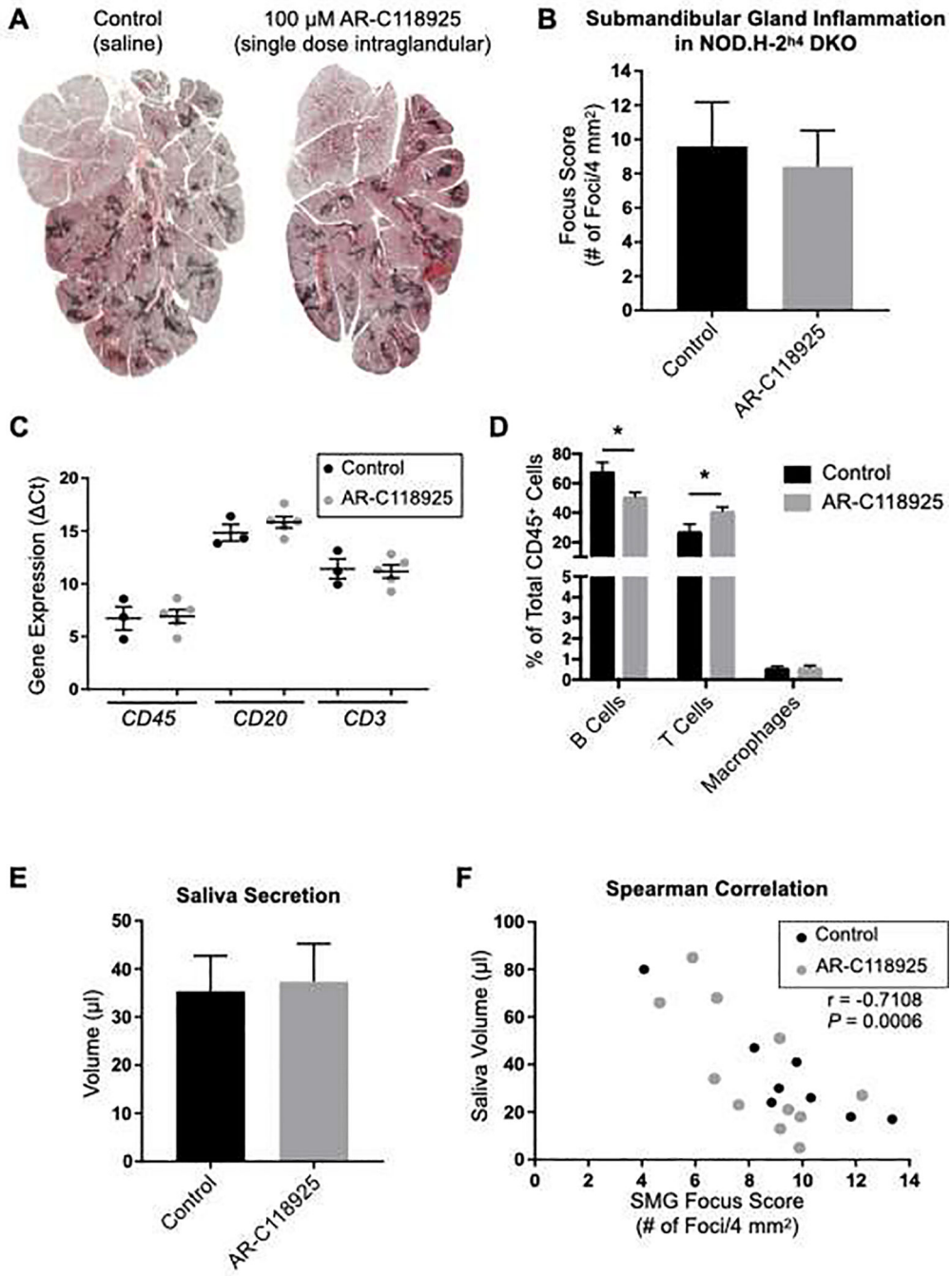

Figure 2. Intraglandular administration of the P2Y$_2$R antagonist AR-C118925 does not resolve sialadenitis in SMGs of NOD.H-2^{h4} DKO mice.

AR-C118925 (30 µl of 100 µM antagonist in saline) or saline (control) was administered in the SMG by intraglandular infusion through the Wharton's ducts of 4.5 month old female NOD.H-2^{h4} DKO mice. After three days, carbachol-induced saliva was collected and SMGs were subjected to histological, qRT-PCR and flow cytometric analyses. (A) Representative images of H&E-stained, formaldehyde-fixed and paraffin-embedded sections of treated SMGs showing lymphocytic foci. (B) Lymphocytic focus score quantification. (C) cDNA prepared from intraglandular AR-C118925- or saline-treated SMGs was subjected to qRT-

PCR analysis using specific primers for the pan immune cell marker *CD45*, the B cell marker *CD20* or the T cell marker *CD3*. A higher ΔCt value indicates lower expression. (D) Immune cells isolated from SMGs of female NOD.H-2^{h4} DKO mice were stained with a panel of fluorophore-conjugated antibodies to identify B cells ($CD45^+$,$CD19^+$), T cells ($CD45^+$,$CD3^+$) and macrophages (CD45+,$F4/80^+$) by flow cytometric analysis. (E) Saliva was collected from control and AR-C118925-treated mice for 15 minutes following i.p. injection of 0.25 mg/kg carbachol. (F) Spearman correlation reveals an inverse relationship between the volume of saliva secretion and focus score in both the AR-C118925- and saline-treated mice. Data are means ± S.E.M. for n = 3 or 5 experiments for qRT-PCR and n = 7 or 8 mice for all other data, where $*P < 0.05$.

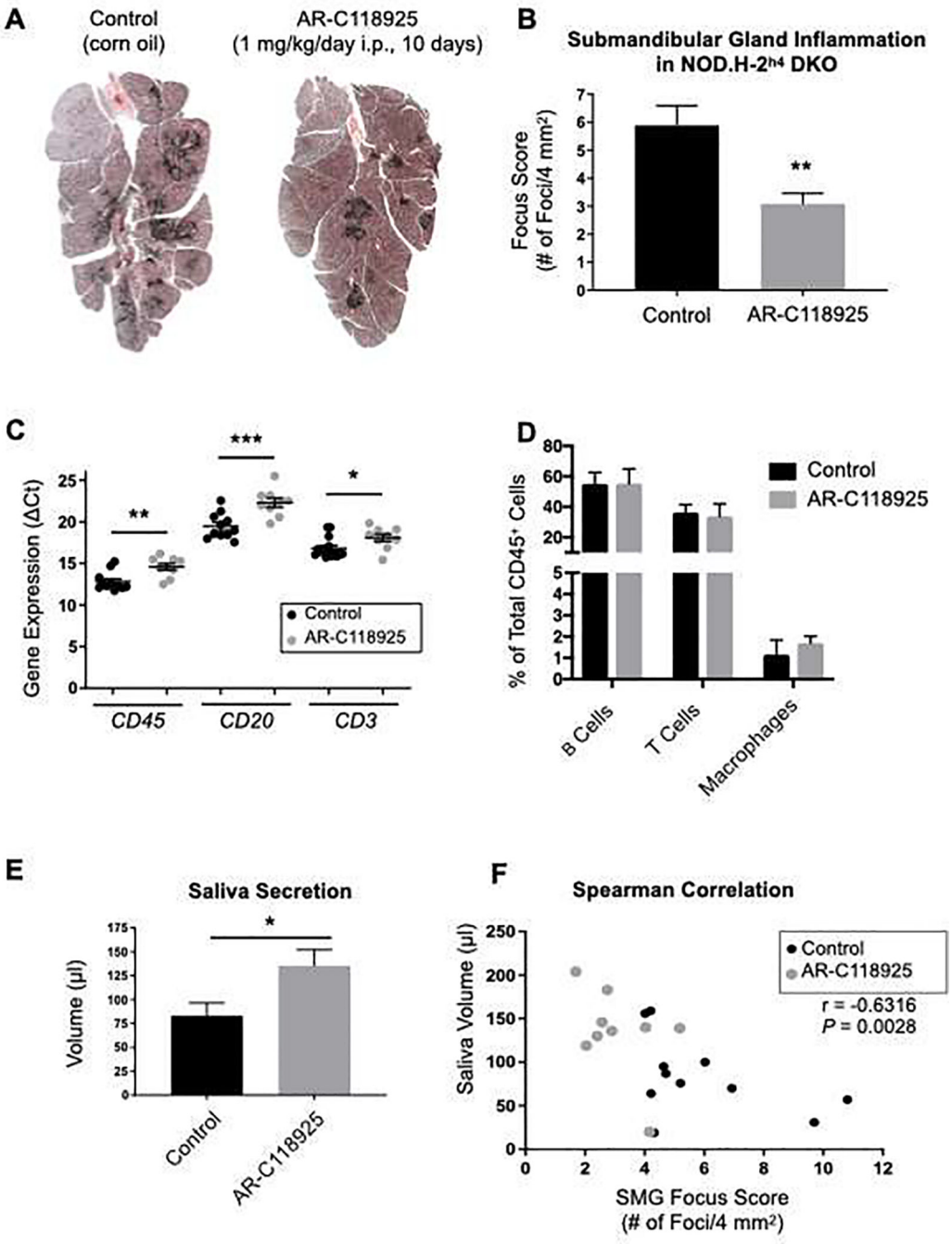

Figure 3. Systemic P2Y$_2$R antagonist AR-C118925 diminishes lymphocytic foci and improves salivation in NOD.H-2^{h4} DKO mice.

AR-C118925 (1 mg/kg/day) or corn oil (control) was administered by daily intraperitoneal injection for 10 days in 4.5 month old female NOD.H-2^{h4} DKO mice. (A) Representative images of H&E-stained, formaldehyde-fixed and paraffin-embedded sections of treated SMGs showing lymphocytic foci. (B) Lymphocytic focus score quantification. (C) cDNA prepared from SMGs of mice treated systemically with AR-C118925 or corn oil was subjected to qRT-PCR analysis using specific primers for the pan immune cell marker *CD45*, the B cell marker *CD20* or the T cell marker *CD3*. A higher ΔCt value indicates

lower expression. (D) Immune cells isolated from SMGs of female NOD.H-2^{h4} DKO mice were stained with a panel of fluorophore-conjugated antibodies to identify B cells ($CD45^+$,$CD19^+$), T cells ($CD45^+$,$CD3^+$) and macrophages ($CD45^+$,$F4/80^+$) by flow cytometric analysis. (E) Saliva was collected from control and AR-C118925-treated mice for 15 minutes following i.p. injection of 0.25 mg/kg carbachol. (F) Spearman correlation reveals an inverse relationship between the volume of saliva secretion and focus score in both the AR-C118925- and vehicle-treated mice. Data are means ± S.E.M. for n = 7 or 8 mice, where $*P < 0.05$, $**P < 0.01$ and $***P < 0.001$.

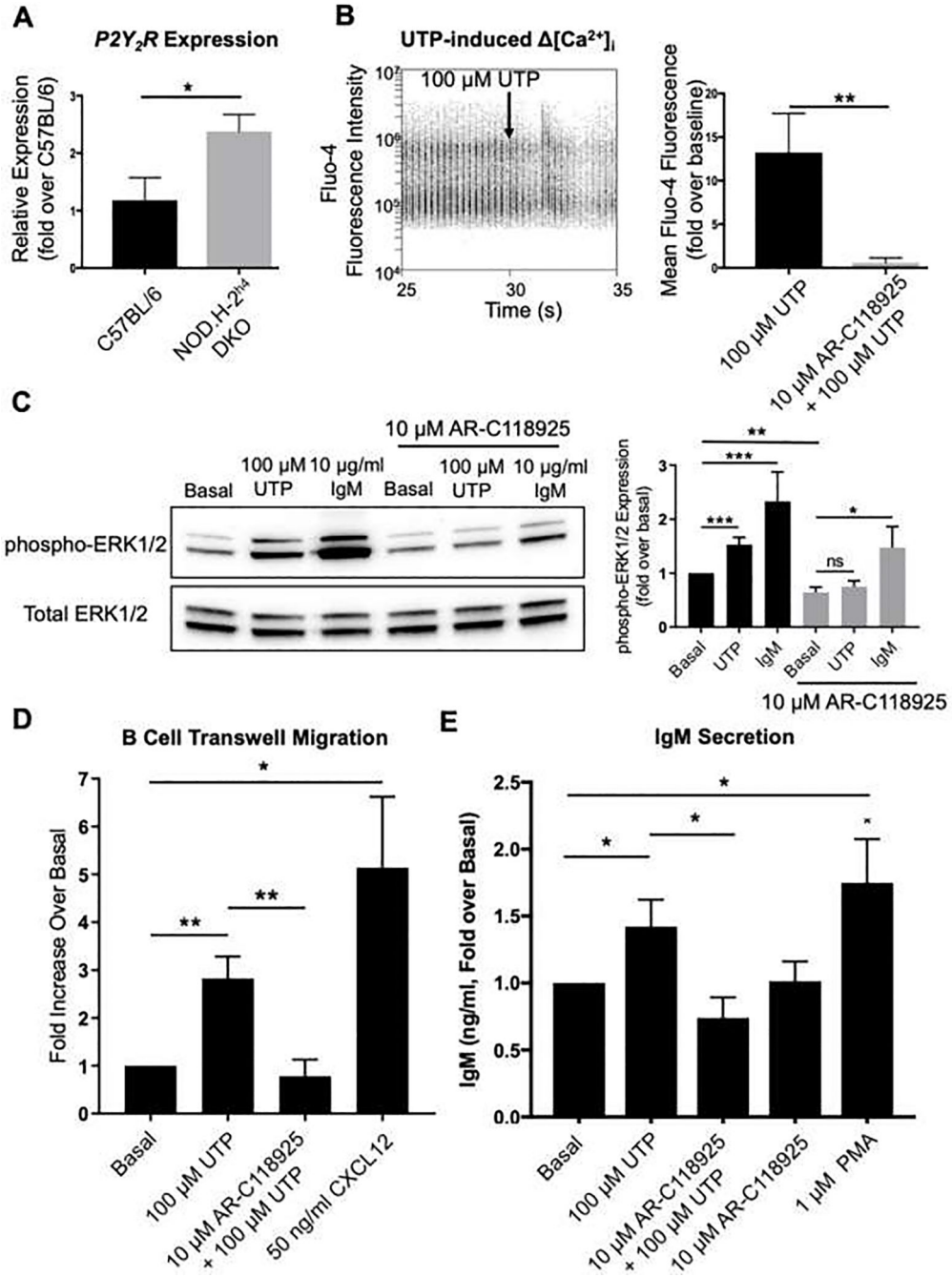

Figure 4. SMG B cells express functional P2Y$_2$R.

(A) Isolated B cells from SMGs of 5 month old female NOD.H-2^{h4} DKO and C57BL/6 mice were subjected to qRT-PCR analysis using specific primers for *P2Y$_2$R*. (B) Dispersed NOD.H-2^{h4} DKO SMG cells were loaded with the Ca^{2+}-sensitive dye Fluo-4 AM and stained with anti-B220 APC-conjugated antibodies to identify B cells, then 100 μM UTP-induced $\Delta[Ca^{2+}]_i$ was determined by continuous measurement of the change in Fluo-4 fluorescence in B220-positive B cells using flow cytometric analysis. UTP-induced $\Delta[Ca^{2+}]_i$ was quantified in B cells treated with or without the P2Y$_2$R antagonist AR-C118925 (10

μM) for 5 minutes. Data are shown as the fold change in mean fluorescence over baseline mean fluorescence. (C) Isolated NOD.H-2^{h4} DKO SMG B cells were pre-treated with or without AR-C118925 (10 μM, 1 hour), then treated for 5 minutes with 100 μM UTP or 10 μg/ml IgM and Western analysis of phospho-ERK1/2 (Thr202/Tyr204) and total ERK1/2 expression was performed. (D) B cells in RPMI media with or without AR-C118925 pre-treatment were placed in the upper well of a Transwell chamber (5 μm pore) and 100 μM UTP or 50 ng/ml CXCL12 was added to the lower chamber. B cell migration into the lower chamber was quantified after 4 h. (E) Following a 1 hour pre-treatment with or without 10 μM AR-C118925, SMG B cells were treated for 72 hours with 100 μM UTP or 1 μM PMA and IgM secretion into the media was measured by ELISA. Data represent means ± S.E.M. for n ≥ 3 experiments, where $*P < 0.05$, $**P < 0.01$ and $***P < 0.001$.